INTERNATIONAL JOURNAL FOR NUMERICAL METHODS IN ENGINEERING
Int. J. Numer. Meth. Engng 2009; **0**:1–16 *Prepared using* nmeauth.cls *[Version: 2002/09/18 v2.02]*

A method for interpolating on manifolds structural dynamics reduced-order models

David Amsallem[1*], Julien Cortial[2], Kevin Carlberg[1] and Charbel Farhat[3]

[1] *Department of Aeronautics and Astronautics*
[2] *Institute for Computational and Mathematical Engineering*
[3] *Vivian Church Hoff Professor of Aircraft Structures, Department of Aeronautics and Astronautics, Department of Mechanical Engineering and Institute for Computational and Mathematical Engineering*
Stanford University, Mail Code 3035, Stanford, CA 94305, U.S.A.

SUMMARY

A rigorous method for interpolating a set of parameterized linear structural dynamics reduced-order models (ROMs) is presented. By design, this method does not operate on the underlying set of parameterized full-order models. Hence, it is amenable to an on-line real-time implementation. It is based on mapping appropriately the ROM data onto a tangent space to the manifold of symmetric positive definite matrices, interpolating the mapped data in this space and mapping back the result to the aforementioned manifold. Algorithms for computing the forward and backward mappings are offered for the case where the ROMs are derived from a general Galerkin projection method and the case where they are constructed from modal reduction. The proposed interpolation method is illustrated with applications ranging from the fast dynamic characterization of a parameterized structural model to the fast evaluation of its response to a given input. In all cases, good accuracy is demonstrated at real-time processing speeds. Copyright © 2009 John Wiley & Sons, Ltd.

KEY WORDS: reduced-order modeling; matrix manifolds; real-time prediction; surrogate modeling; linear structural dynamics

1. INTRODUCTION

The concept of model reduction is old in structural dynamics. It has — and is still — been used for many purposes ranging from the design of a test-analysis model to provide a basis for comparing computational and experimental results, to the alleviation of the computational burden associated with large-scale finite element models. Among the many linear model reduction techniques that have been or remain popular in industry, one can mention Guyan's

*Correspondence to: Department of Aeronautics and Astronautics, Stanford University, Mail Code 3035, Stanford, CA 94305, U.S.A.

Contract/grant sponsor: Air Force Office of Scientific Research; contract/grant number: 49620-01-1-0129

Contract/grant sponsor: National Science Foundation; contract/grant number: 0540419

reduction method [1] and the related superelement dynamic reduction approaches, the IRS dynamic reduction method [2], and of course, the ubiquitous modal reduction method. More recently, the Proper Orthogonal Decomposition (POD) [3] method, which can be used to generate a reduced-order model (ROM) capable of accurately reproducing the dynamics of the underlying full-order model for a given set of input forces, has gained status in the linear structural dynamics community [4, 5, 6]. All of these methods can be described as Galerkin projection techniques onto carefuly chosen reduced-order bases. They are back in vogue for incorporating computational models in design operations [7], designing effective control systems for large-scale flexible structures [8], generating surrogate models for accelerating the speed of optimization procedures [9] and developing realistic uncertainty quantification analysis methods [10]. In all of these applications, structural dynamics ROMs are sought after because of their potential for operating in real-time.

Unfortunately in all of the above and many other applications, structural dynamics models are usually parameterized, their reduced-order counterparts tend to lack robustness[12, 11] with respect to parameter changes, and the reconstruction of these small-size counterparts for each new set of parameters can be computationally prohibitive. Hence, there is a pressing need for a fast ROM adaptation procedure which can operate on-line and in real-time. Here, on-line characterizes a procedure which does not operate on the full-order model at the origin of a ROM and therefore which avoids the manipulation of a large-scale complex simulation software and the associated implementation burden. The real-time requirement is to preserve the reason why ROMs are desired in the first place for the target applications — that is, computational speed.

To develop a structural dynamics ROM adaptation procedure that meets the aforementioned requirements, a database of reduced-order information can be precomputed for selected values of the parameter set and interpolation can be invoked for generating ROMs for other values of this parameter set. However, it turns out that interpolating reduced-order data is not an easy task. For example, reduced-order bases are often orthogonal and the straightforward interpolation of sets of orthogonal vectors does not necessarily generate a new set of orthogonal vectors. Similarly, the straightforward interpolation of ROMs does not necessarily yield a ROM. This is because neither reduced-order bases nor ROMs live in vector spaces.

Most recently, a numerical method based on interpolation in a tangent space to the Grassmann manifold was developed for adapting CFD (computational fluid dynamics)-based reduced-order POD bases to parameter changes in real-time [11, 13]. However, the application of such a method to the interpolation of projection-based ROMs can neither be performed on-line nor in real-time, because it requires first evaluating the underlying full-order model at the new value of the parameter set, then projecting this model onto the interpolated reduced-order basis. In this work, the symmetric positive definite nature of linear structural dynamics models is exploited to develop an interpolation method which directly operates on linear structural dynamics ROMs rather than on their associated reduced-order bases and therefore can be implemented on-line and perform in real-time. To this effect, the remainder of this paper is organized as follows.

In Section 2, the representation of a linear structural dynamic ROM is abstracted and the ROM adaptation problem is formulated. In Section 3.2, a method based on mapping appropriately the ROM data onto a tangent space to the manifold of symmetric positive definite matrices of size n, $\mathrm{SPD}(n)$, interpolating the mapped data in this space and mapping back the result to the aforementioned manifold is presented. Algorithms for computing the

forward and backward mappings are offered in Section 3.3.1 for the special case where the ROMs are constructed by modal reduction and in Section 3.3.2 for the case where they are constructed by a general Galerkin projection method. The proposed interpolation method is illustrated in Section 4 with simple applications which nevertheless highlight its ability to deliver good accuracy at real-time processing speeds.

2. PROBLEM FORMULATION

In this work, a parameterized linear structural dynamics (full-order) model of size N is abstracted as a triplet of the form

$$\big(M(s),\ C(s),\ K(s)\big) \in \big(\mathbb{R}^{N\times N},\ \mathbb{R}^{N\times N},\ \mathbb{R}^{N\times N}\big), \tag{1}$$

where M, C and K are symmetric positive definite mass, damping and stiffness matrices, respectively, and $s = (s_0, s_1, \ldots, s_{N_p-1})$ denotes a set of N_p model parameters. These parameters can be physical, non-physical, or a combination of both.

Similarly, a corresponding ROM of size $n << N$ is abstracted here as

- A1: a triplet of reduced mass, damping and stiffness matrices that are assumed here to be symmetric positive definite

$$R(s) = \big(M^\star(s),\ C^\star(s),\ K^\star(s)\big) \in \big(\mathbb{R}^{n\times n},\ \mathbb{R}^{n\times n},\ \mathbb{R}^{n\times n}\big), \tag{2}$$

or

- A2: a quintuplet of the form

$$R(s) = \big(M^\star(s),\ C^\star(s),\ K^\star(s),\ X(s),\ Z(s)\big) \in \big(\mathbb{R}^{n\times n},\ \mathbb{R}^{n\times n},\ \mathbb{R}^{n\times n},\ \mathbb{R}^{N\times n},\ \mathbb{R}^{N\times n}\big), \tag{3}$$

where

$$\begin{aligned} M^\star(s) &= X^T(s)M(s)X(s), \quad & C^\star(s) &= X^T(s)C(s)X(s), \\ K^\star(s) &= X^T(s)K(s)X(s), & Z(s) &= A(s)X(s), \end{aligned} \tag{4}$$

$A \in \mathbb{R}^{N\times N}$ is a real symmetric positive definite matrix, $X(s)$ denotes a projection matrix relating the full- and reduced-order displacement vectors $u \in \mathbb{R}^N$ and $q \in \mathbb{R}^n$ via

$$u(t,s) = X(s)q(t,s) \tag{5}$$

and satisfying the orthogonality condition

$$X^T(s)Z(s) = I_n, \tag{6}$$

t denotes time, $I_n \in \mathbb{R}^{n\times n}$ is the identity matrix of size n and the superscript T designates the transpose operation.

Indeed, the governing equations associated with a linear structural dynamics ROM can be written in general as

$$M^\star(s)\ddot{q}(t,s) + C^\star(s)\dot{q}(t,s) + K^\star(s)q(t,s) = F^\star(t,s), \tag{7}$$

where a dot designates a time derivative. Hence, definition A1 is appropriate when the loading on the structure is not of any particular interest and therefore $F^\star(t,s) = 0$ — for example, when

the main interest is in determining a set of natural frequencies of the full-order parameterized structural model. In this case, $M^\star$, $C^\star$ and $K^\star$ do not necessarily result from a projection technique but are assumed here to be symmetric positive definite. Definition A2 is appropriate as soon as $F^\star(t,s) \neq 0$ or the mapping between $u(t,s)$ and $q(t,s)$ is required. It covers most linear ROMs constructed by popular projection techniques where $X(s) \in \mathbb{R}^{N\times n}$ is a real rectangular matrix whose columns form a reduced-order basis and $A(s)$ is associated with a metric. In this case, $F^\star(t,s) = X^T(s)F(t)$ and $X(s)$ satisfies an orthogonality constraint. For example, when $X(s)$ is generated by the POD method, this matrix satisfies $X^T(s)X(s) = I_n$ and therefore $A(s) = I_N$. Alternatively, $X(s)$ can be a set of eigenvectors of the pencil $\big(M(s),\ K(s)\big)$, in which case $A(s) = M(s)$ and therefore the ROM is essentially a truncated modal representation of the structure. In all cases, $M^\star$, $C^\star$ and $K^\star$ are symmetric positive definite and therefore belong to the manifold $\mathrm{SPD}(n)$.

Using the above nomenclature, the focus of this paper is on solving the following problem.

Problem. Let $s^{(i)} = \big(s_0^{(i)},\, s_1^{(i)},\, \ldots,\, s_{N_p-1}^{(i)}\big)$ denote a specific configuration of the set of N_p parameters s. In the remainder of this paper, $s^{(i)}$ is referred to as the $(i+1)$-th point of a set of operating points

$$S = \big(s^{(0)},\, s^{(1)},\, \ldots,\, s^{(N_R-1)}\big). \tag{8}$$

Let also $\{R_i\}_{i=0}^{N_R-1} = \big\{R\big(s^{(i)}\big)\big\}_{i=0}^{N_R-1}$ denote a set of N_R linear structural dynamics ROMs of the same dimension n constructed at the operating points $\big\{s^{(i)}\big\}_{i=0}^{N_R-1}$. Given a new operating point $s^{(N_R)} \notin S$, compute on-line and in real-time $R_{N_R} = R\left(s^{(N_R)}\right)$.

The remainder of this paper proposes a solution to the above problem based on a suitable interpolation method.

3. ROM ADAPTATION METHODS

Three different but related ROM adaptation methods are presented here: one for the case where the ROMs $\{R_i\}_{i=0}^{N_R-1}$ are of type A1 and two for the case where they are of type A2. All three methods share the concept of interpolation in a tangent space to a manifold. Unlike any straightforward interpolation scheme, this concept enables all three methods to produce for any new operating point $s^{(N_R)}$ a result $R\big(s^{(N_R)}\big)$ that is a *genuine* ROM — that is, a result R_{N_R} whose matrices $M^\star\big(s^{(N_R)}\big)$, $C^\star\big(s^{(N_R)}\big)$ and $K^\star\big(s^{(N_R)}\big)$ are symmetric positive definite and whose matrix $X\big(s^{(N_R)}\big)$ in the case of type A2 satisfies the constraints $\big(6\big)$. All of these methods are based on the approach presented in Section 3.1 which can be summarized as follows: first, the data to be interpolated is mapped appropriately onto a tangent space to the appropriate manifold, then the mapped data is interpolated in this space and finally the interpolation result is mapped back to the same manifold (see Figure 1).

For a background on interpolation in a tangent space to a manifold, the reader can consult references [11, 13], among others.

3.1. Interpolation in a Tangent Space to a Manifold

Let $\big\{\mathcal{Y}_i = \mathcal{Y}\big(s^{(i)}\big)\big\}_{i=0}^{N_R-1}$ denote a set of elements of a manifold $\mathcal{M}$ associated with a set of different operating points $\{s^{(i)}\}_{i=0}^{N_R-1}$. Each element $\mathcal{Y}_i$ is represented here by a matrix

$Y_i \in \mathbb{R}^{m\times p}$ that belongs to some matrix manifold $\mathcal{M}'$ and verifies one or more specific properties that characterize $\mathcal{M}'$. (The m-dimensional sphere, $\mathbb{S}^m$, the group of orthogonal matrices of size m, $\mathcal{O}(m)$, and the set of symmetric positive matrices of size m SPD(m) are examples of simple matrix manifolds.) The following four-step method is proposed to construct a new element $\mathcal{Y}_{N_R} \in \mathcal{M}$ associated with a new operating point $s^{(N_R)}$ and its representative matrix Y_{N_R} — that is, an element $\mathcal{Y}_{N_R} \in \mathcal{M}$ and its representative matrix $Y_{N_R} \in \mathcal{M}'$ which have the same properties as each element $\mathcal{Y}_i$ and its representative matrix $Y_i,\ i = 0, ..., N_R - 1$, respectively.

- Step 0. Choose an element $\mathcal{Y}_{i_0}$ in the data set $\{\mathcal{Y}_i\}_{i=0}^{N_R-1}$ as a reference element of the manifold $\mathcal{M}$.
- Step 1. Consider a few elements of the set $\{\mathcal{Y}_i\}_{i=0}^{N_R-1}$ that lie in a neighborhood of $\mathcal{Y}_{i_0}$. Map each of them onto the tangent space to $\mathcal{M}$ at $\mathcal{Y}_{i_0}$ denoted here by $\mathcal{T}_{\mathcal{Y}_{i_0}}\mathcal{M}$. More specifically, map each element $\mathcal{Y}_i$ that is sufficiently close to $\mathcal{Y}_{i_0}$ to an element $\chi_i \in \mathcal{T}_{\mathcal{Y}_{i_0}}\mathcal{M}$ represented by a matrix Γ_i, using the logarithm map $\mathrm{Log}_{\mathcal{Y}_{i_0}}$ which provides an appropriate continuous mapping to the tangent space of the manifold at $\mathcal{Y}_{i_0}$. This can be written as:

$$\chi_i = \mathrm{Log}_{\mathcal{Y}_{i_0}}(\mathcal{Y}_i). \tag{9}$$

- Step 2. Compute each entry of an $m \times p$ matrix Γ_{N_R} associated with the target operating point $s^{(N_R)}$ by interpolating the corresponding entries of the $m \times p$ matrices $\{\Gamma_i\}$ associated with the operating points $\{s^{(i)}\}$ using any preferred multi-variate interpolation algorithm.
- Step 3. Map the element $\chi_{N_R} \in \mathcal{T}_{\mathcal{Y}_{i_0}}\mathcal{M}$ represented by the matrix Γ_{N_R} to an element $\mathcal{Y}_{N_R} \in \mathcal{M}$ represented by a matrix $Y_{N_R} \in \mathcal{M}'$ using the exponential map $\mathrm{Exp}_{\mathcal{Y}_{i_0}}$. This can be written as

$$\mathcal{Y}_{N_R} = \mathrm{Exp}_{\mathcal{Y}_{i_0}}(\chi_{N_R}). \tag{10}$$

In the remainder of this paper, the above method is referred to as the "generalized" (because it involves more than) interpolation of a set of elements $\{\mathcal{Y}_i\}$ in a tangent space to a matrix manifold $\mathcal{M}$. The specific algorithms for computing the logarithm and exponential mappings depend of the manifold $\mathcal{M}$ and are discussed next.

3.2. Case A1

Here, $\mathcal{M} = \mathcal{M}' = \mathrm{SPD}(n)$ as the triplets of interest

$$R_i = \left(M^\star(s^{(i)}),\ C^\star(s^{(i)}),\ K^\star(s^{(i)})\right) \in \left(\mathbb{R}^{n\times n},\ \mathbb{R}^{n\times n},\ \mathbb{R}^{n\times n}\right),\quad i = 0, ..., N_R - 1 \tag{11}$$

are constituted of symmetric positive definite matrices. In this case, the matrix logarithm and exponential mappings are given by[14]

$$\mathrm{Log}_{Y_{i_0}}(Y_i) = \texttt{logm}\left(Y_{i_0}^{-1/2} Y_i Y_{i_0}^{-1/2}\right) \tag{12}$$

and

$$\mathrm{Exp}_{Y_{i_0}}(\Gamma) = Y_{i_0}^{1/2}\texttt{expm}(\Gamma)Y_{i_0}^{1/2}, \tag{13}$$

where `logm` and `expm` denote the matrix logarithm and exponential, respectively.

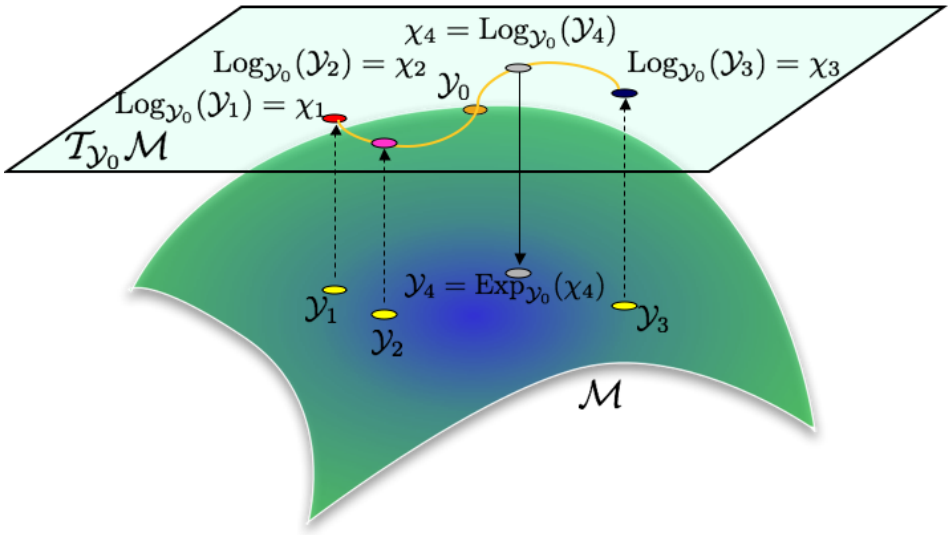

Figure 1. Graphical description of the generalized interpolation of the matrices $\{Y_i\}_{i=0}^3$ in a tangent space to a matrix manifold $\mathcal{M}$.

REMARK. In the particular case where the interpolation data of the form given in (2) is based on the classical modal decomposition and truncation method, $M^\star\big(s^{(i)}\big) = I_n$ and $K^\star\big(s^{(i)}\big) = \Omega_n^2\big(s^{(i)}\big)$, where Ω_n^2 is a diagonal matrix of squares of n natural circular frequencies. In this case, the generalized interpolation method described above preserves the structure of the interpolation triplets $\Big(I_n,\ C^\star\big(s^{(i)}\big),\ \Omega_n^2\big(s^{(i)}\big)\Big)$ as it generates a pair of reduced-order matrices $M^\star\big(s^{(N_R)}\big)$ and $K^\star\big(s^{(N_R)}\big)$ that satisfy $M^\star\big(s^{(N_R)}\big) = I_n$ and $K^\star\big(s^{(N_R)}\big) = \Omega_n^2\big(s^{(N_R)}\big)$, where Ω_n^2 is a diagonal matrix with n positive entries. This important property of the proposed generalized interpolation method in a tangent space to a matrix manifold is proven in the Appendix in Section 6 of this paper.

3.3. Case A2

Here, the quintuplets of interest

$$R_i = \big(M^\star(s^{(i)}),\ C^\star(s^{(i)}),\ K^\star(s^{(i)}),\ X(s^{(i)}),\ Z(s^{(i)})\big) \in \big(\mathbb{R}^{n\times n},\ \mathbb{R}^{n\times n},\ \mathbb{R}^{n\times n},\ \mathbb{R}^{N\times n},\ \mathbb{R}^{N\times n}\big), \tag{14}$$

for $i = 0, ..., N_R - 1$, are constituted of three symmetric positive definite matrices and two rectangular matrices representing two reduced-order bases and satisfying the constraint (6). The three square matrices belong to the manifold SPD(n) as in the previous case. The two subspaces spanned by the columns of $X(s^{(i)})$ and $Z(s^{(i)})$ belong to the Grassmann manifold $\mathcal{G}(n, N)$, which is defined as the set of subspaces of dimension n in $\mathbb{R}^N$.

Hence, in this case, the matrix logarithm and exponential mappings to be used for interpolating the matrices $\{M^\star(s^{(i)})\}$, the matrices $\big\{C^\star\big(s^{(i)}\big)\big\}$ and the matrices $\big\{K^\star\big(s^{(i)}\big)\big\}$ are the same as in Case A1.

The computation of the two matrices $X\left(s^{(N_R)}\right)$ and $Z\left(s^{(N_R)}\right)$ requires the generalized interpolation of two different sets of matrices $\left\{X\left(s^{(i)}\right)\right\}$ and $\left\{Z\left(s^{(i)}\right)\right\}$ that are however connected by the orthogonality condition (6). Hence, this computation cannot be performed using the generalized interpolation method presented in Section 3.1 as is. Instead, it is proposed to simultaneously interpolate the set of matrices $X\left(s^{(i)}\right)$ and set of matrices $Z\left(s^{(i)}\right)$ column-block per column-block while enforcing the orthogonality constraint (6). For this purpose, two sub-cases are distinguished: the sub-case where $X\left(s^{(N_R)}\right)$ is associated with the classical modal decomposition and truncation method and that where $X\left(s^{(N_R)}\right)$ is associated with an arbitrary Galerkin projection method.

3.3.1. Modal Truncation The modal truncation approach differs from the general Galerkin projection approach in that each individual column of a matrix $X(s^{(i)})$ has a specific meaning and importance that must be preserved during the interpolation process. More specifically, if the columns of the matrices $\left\{X\left(s^{(i)}\right)\right\}$ to be interpolated are ordered so that the j-th column of each of them refers to the same eigenmode, then the j-th column of the interpolated matrix $X\left(s^{(N_R)}\right)$ must refer to the same eigenmode. This is not true however for a set of matrices $\left\{X\left(s^{(i)}\right)\right\}$ associated with an arbitrary Galerkin projection method. Therefore, the generalized interpolation method proposed here loops on the eigensubspaces $\left\{\mathcal{S}_{ij}^X\right\}$ and subspaces $\left\{\mathcal{S}_{ij}^Z\right\}$ $\left(\text{where } i \text{ refers to } s^{(i)}\right)$ of the parameterized system underlying all matrices $\left\{X\left(s^{(i)}\right)\right\}$ and $\left\{Z\left(s^{(i)}\right)\right\}$ and interpolates each of such set of matrices while enforcing the orthogonality constraint (6) as described below. For clarity, the proposed generalized interpolation method is first described in the simple case where each eigensubspace is of dimension 1. In this case, $\mathcal{S}_{ij}^X \in \mathcal{G}(1,N)$ and $\mathcal{S}_{ij}^Z \in \mathcal{G}(1,N)$.

For $j = 1, \ldots, n$

- Step 0. Interpolate the eigensubspaces $\left\{\mathcal{S}_{ij}^X \in \mathcal{G}(1,N)\right\}$ using the generalized interpolation algorithm described in Section 3.1 with $\mathcal{M} = \mathcal{G}(1,N)$ and $\mathcal{M}'$ the non compact Stiefel manifold of non zero vectors of size N. The matrix logarithm and exponential mappings associated with $\mathcal{G}(1,N)$ are given by

$$\left(I_N - X_{i_0 j}\left(X_{i_0 j}^T X_{i_0 j}\right)^{-1} X_{i_0 j}^T\right) X_{ij}\left(X_{i_0 j}^T X_{ij}\right)^{-1}\left(X_{i_0 j}^T X_{i_0 j}\right)^{\frac{1}{2}} = U\Sigma V^T \qquad \text{(Thin SVD)} \tag{15}$$

$$\mathrm{Log}_{\mathcal{S}_{i_0 j}}(\mathcal{S}_{ij}) = \mathrm{span}\left(U \tan^{-1}(\Sigma) V^T\right) \tag{16}$$

and

$$\Gamma = U\Sigma V^T \qquad \text{(Thin SVD)} \tag{17}$$

$$\mathrm{Exp}_{\mathcal{S}_{i_0 j}}(\chi) = \mathrm{span}\left(X_{i_0 j}\left(X_{i_0 j}^T X_{i_0 j}\right)^{-\frac{1}{2}} V\cos(\Sigma) + U\sin(\Sigma)\right), \tag{18}$$

where X_{ij} denotes the j-th column of $X\left(s^{(i)}\right)$.

- Step 1. Perform a Gram-Schmidt procedure on $X_{N_R j}$ to enforce the orthogonality conditions $X_{N_R j}^T Z_{N_R l} = 0, \quad l = 1, \ldots, j-1$, where Z_{ij} denotes the j-th column of $Z\left(s^{(i)}\right)$.

- Step 2. Interpolate the subspaces $\left\{\mathcal{S}_{ij}^{Z} \in \mathcal{G}(1,N)\right\}$ using the generalized interpolation algorithm described in Section 3.1 with $\mathcal{M} = \mathcal{G}(1,N)$ and $\mathcal{M}'$ the non compact Stiefel manifold of non zero vectors of size N.
- Step 4. Perform a Gram-Schmidt procedure on $Z_{N_R j}$ to enforce the orthogonality conditions $X_{N_R l}^T Z_{N_R j} = 0, \;\; l = 1, \ldots, j-1$ and $X_{N_R j}^T Z_{N_R j} = 1$.
- Step 5. Scale $X_{N_R j}$ and $Z_{N_R j}$ so that their two-norms are comparable to the two-norms of $\{X_{ij}\}$ and $\{Z_{ij}\}$, respectively.

The extension of the above generalized interpolation algorithm to the case where each eigensubspace $\{\mathcal{S}_{ij}^{X}\}$ is of the same dimension $k_j > 1$ is straightforward. The extension to the case where k_j is variable requires book keeping.

3.3.2. Arbitrary Galerkin Projection In this case, the proposed generalized interpolation method is identical to that described in the previous section for $k_j = 1$.

4. APPLICATIONS

Here, the proposed interpolation method is illustrated with two simple applications that highlight its potential for adapting on-line a structural dynamics ROM to a new operating point.

4.1. Case A1: a Mass-Damper-Spring System

The dynamic equations of equilibrium governing the mass-damper-spring system shown in Figure 2 (and previously studied by Kim [15]) can be reduced by Galerkin projection and written in state-space form as follows

$$\dot{z}(t,s) = H(s) z(t,s) + b(s), \tag{19}$$

where

$$z(t,s) = \begin{bmatrix} \dot{q}(t,s) \\ q(t,s) \end{bmatrix}, \quad H(s) = \begin{bmatrix} -M^\star(s)^{-1} C^\star(s) & -M^\star(s)^{-1} K^\star(s) \\ I_n & 0_n \end{bmatrix}, \quad b(s) = \begin{bmatrix} M^\star(s)^{-1} F^\star(s) \\ 0 \end{bmatrix} \tag{20}$$

and 0_n denotes the zero matrix of size n, where n denotes the size of the reduced-order basis.

Each operating point of this mechanical system consists of $3p$ parameters corresponding to the $3p$ values of the masses $\{m_j\}_{j=1}^p$, dampers $\{c_j\}_{j=1}^p$ and springs $\{k_j\}_{j=1}^p$. However for the sake of simplicity, it is assumed here that: $\forall j = 1, \ldots, p, \;\; m_j = m, \;\; c_j = c, \;$ and $k_j = k$, so that each operating point is uniquely defined by the three parameters (m, c, k), only.

The system is here constituted of $p = 24$ mass-damper-spring units. Using the POD method as described by Kim [15], four different reduced-order bases $\{\Phi_i\}_{i=0}^3$ of dimension $n = 10$ each are generated for the four different operating points $\{s^{(i)}\}_{i=0}^3$ defined in Table I. These bases are then used to precompute four different sets of reduced-order matrices $\left\{M^\star\left(s^{(i)}\right), C^\star\left(s^{(i)}\right), K^\star\left(s^{(i)}\right)\right\}_{i=0}^3$. Table I also specifies a fifth operating point $s^{(4)}$ for which no reduced-order data is precomputed.

Hence, the reduced-order matrices $M^\star\left(s^{(4)}\right)$, $C^\star\left(s^{(4)}\right)$ and $K^\star\left(s^{(4)}\right)$ are next computed via two different approaches: (a) using the generalized matrix interpolation method proposed in

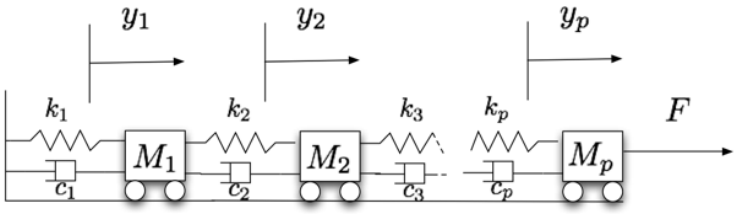

Figure 2. Mass-damper-spring system.

Table I. Five operating points of a mass-damper-spring system.

	m	c	k
$s^{(0)}$	0.3	0.6	0.7
$s^{(1)}$	0.7	0.6	1.3
$s^{(2)}$	0.9	0.6	1.0
$s^{(3)}$	1.1	0.6	0.4
$s^{(4)}$	0.8	0.6	1.1

this paper and (b) by generating first a new POD basis Φ_4 for the operating point $s^{(4)}$ and then projecting the full-order matrices $M\big(s^{(4)}\big)$, $C\big(s^{(4)}\big)$ and $K\big(s^{(4)}\big)$ onto this basis. In both cases, the matrix $H(s^{(4)})$ is next constructed and its eigenvalues are computed. These are graphically reported in Figure 3 which reveals that the eigenvalues of the interpolated ROM matrix $H(s^{(4)})$ are in good agreement with those of its directly constructed counterpart.

4.2. Case A2: the AGARD Wing 445.6

The AGARD Wing 445.6[16] is considered here and represented by an undamped ($C = 0$) finite element (FE) model composed of 800 shell elements that generate 2646 degrees of freedom. The geometry of the wing is parameterized by four shape parameters as shown in Figure 4: the root chord c_{root}, the tip chord c_{tip}, the half span length $\dfrac{\bar{s}}{2}$ and the quarter-chord sweep angle $\Lambda_{c/4}$.

A database of linear structural dynamics ROMs is constructed for this wing by precomputing a set of 17 quintuplets $\big\{R\big(s^{(i)}\big) = \big(M^\star(s^{(i)}),\ C^\star(s^{(i)}),\ K^\star(s^{(i)}),\ X(s^{(i)}),\ Z(s^{(i)})\big)\big\}_{i=0}^{16}$ for 17 different design points $\{s^{(i)}\}_{i=0}^{16}$ that can be viewed as the vertices and center of a hypercube in a design space — that is, a subset of $\mathbb{R}^4$ — defined by

$$c_{root} \times c_{tip} \times \frac{\bar{s}}{2} \times \Lambda_{c/4} \in \left[c_{root}^{(min)}, c_{root}^{(max)}\right] \times \left[c_{tip}^{(min)}, c_{tip}^{(max)}\right] \times \left[\frac{\bar{s}^{(min)}}{2}, \frac{\bar{s}^{(max)}}{2}\right] \times \left[\Lambda_{c/4}^{(min)}, \Lambda_{c/4}^{(max)}\right], \tag{21}$$

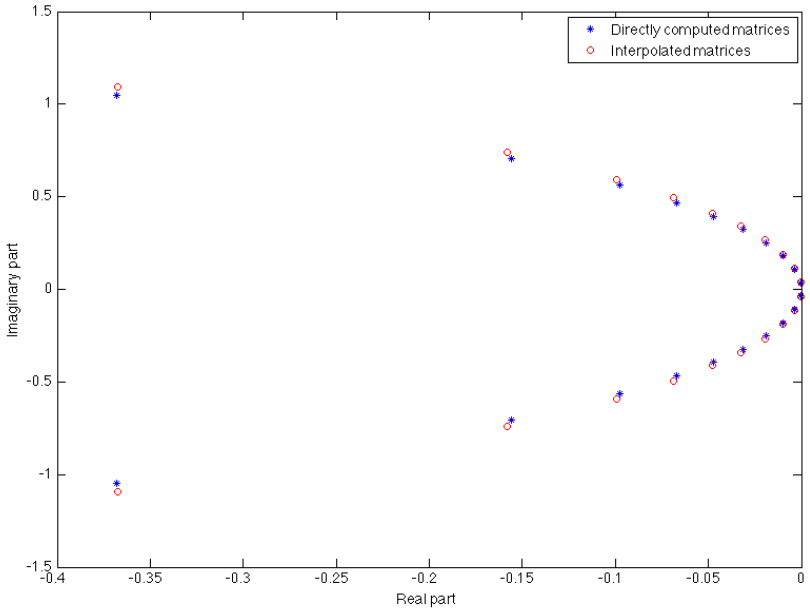

Figure 3. Comparison of the eigenvalues of the reduced-order matrix $H(s^{(4)})$ constructed using the generalized interpolation method and those of its counterpart assembled from directly constructed ROMs.

Table II. AGARD Wing 445.6: bounds of the parametric domain of interest.

$c_{root}^{(min)}$	$c_{root}^{(max)}$	$c_{tip}^{(min)}$	$c_{tip}^{(max)}$	$\bar{s}^{(min)}/2$	$\bar{s}^{(max)}/2$	$\Lambda_{c/4}^{(min)}$	$\Lambda_{c/4}^{(max)}$
17.568 in	26.352 in	11.6 in	17.4 in	24 in	36 in	38.66°	50.16°

where the values of the upper and lower bounds are defined in Table II.

For each of these 17 sample design points, a ROM is constructed by the method of modal decomposition and truncation based on the first five natural modes of this design. Hence, in this case,

$$\left\{R\big(s^{(i)}\big) = \big(I_5,\ 0_5,\ \Omega_5^2(s^{(i)}),\ X(s^{(i)}),\ Z(s^{(i)})\big)\right\}_{i=0}^{16}, \tag{22}$$

where $\Omega_5^2(s)$ denotes the diagonal matrix storing the squares of the first five natural circular frequencies of the structural model of the wing for the design point s.

Here, the accuracy of the generalized interpolation method proposed in this paper is assessed for three arbitrary design points (or configurations), $s^{(a)}$, $s^{(b)}$ and $s^{(c)}$. These design configurations are shown in Figure 5, specified in Table III and referred to in the remainder of this section as "test" design points for the proposed generalized interpolation method. In

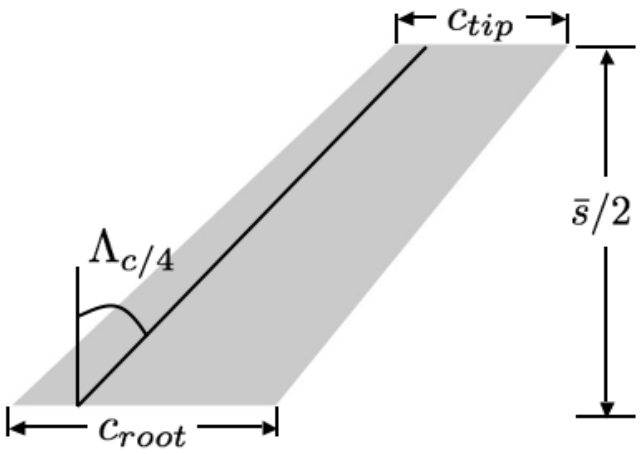

Figure 4. Geometrical parameterization of the AGARD Wing 445.6.

particular, these test design points are sufficiently "far" from the other design points for which reduced-order data is precomputed and stored in the database. Indeed, Table III reports for each parameter of each test design configuration the distance $\delta_\mu\big(s^{(m)}\big)$, $m = \ a,\ b,\ c$, to the precomputed design points defined as

$$\delta_\mu\big(s^{(m)}\big) = \min_{0\le i\le 16} \frac{\big|\mu\big(s^{(m)}\big) - \mu\big(s^{(i)}\big)\big|}{\Big|\max\limits_{0\le i\le 16} \mu\big(s^{(i)}\big) - \min\limits_{0\le i\le 16} \mu\big(s^{(i)}\big)\Big|} \ . \tag{23}$$

More specifically, the 17 precomputed quintuplets of reduced-order matrices and mode shape vectors (22) associated with the 17 precomputed design points are interpolated to generate three similar quintuplets of reduced-order matrices and mode shape vectors associated with the three design points $s^{(a)}$, $s^{(b)}$ and $s^{(c)}$, respectively. To this effect, the reader is reminded that the proposed generalized interpolation method preserves the structure of a diagonal matrix (see the Appendix in Section 6). Hence, it is guaranteed to deliver quintuplets of the form given in (22) when applied to precomputed quintuplets of the same form and as such is a viable alternative approach to the straightforward interpolation of scalar natural frequencies.

The accuracy of the interpolation is first assessed by comparing the natural frequencies and mode shapes of each interpolated linear structural dynamics ROM with those of its directly computed counterpart. For the mode shape vectors, the comparison is performed using the Modal Assurance Criterion [17]. To this effect, the results reported in Table IV and Table V reveal that the eigen characteristics of the interpolated ROMs are in good agreement with those of the directly computed ROMs, thereby illustrating the accuracy of the proposed generalized interpolation method.

Next, the accuracy of the proposed generalized interpolation method is assessed by computing the dynamic response of each test design point of the wing to a sudden and

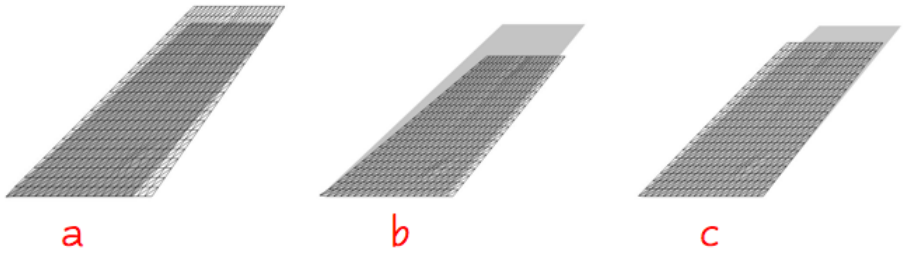

Figure 5. "Test" design points: shaded geometry corresponds to the wing configuration for the values of the shape parameters at the center of the hypercube and geometry shown in wireframe corresponds to the "test" wing configuration.

Table III. "Test" design points.

	c_{root}	c_{tip}	$\bar{s}/2$	$\Lambda_{c/4}$
$s^{(a)}$	25.484 in $\delta_{c_{root}}(s^{(a)}) = 0.099$	15.715 in $\delta_{c_{tip}}(s^{(a)}) = 0.21$	32.852 in $\delta_{\bar{s}/2}(s^{(a)}) = 0.24$	42.21° $\delta_{\Lambda_{c/4}}(s^{(a)}) = 0.19$
$s^{(b)}$	23.414 in $\delta_{c_{root}}(s^{(b)}) = 0.17$	13.549 in $\delta_{c_{tip}}(s^{(b)}) = 0.16$	24.200 in $\delta_{\bar{s}/2}(s^{(b)}) = 0.02$	47.76° $\delta_{\Lambda_{c/4}}(s^{(b)}) = 0.21$
$s^{(c)}$	22.056 in $\delta_{c_{root}}(s^{(c)}) = 0.01$	17.398 in $\delta_{c_{tip}}(s^{(c)}) = 3 \times 10^{-4}$	26.915 in $\delta_{\bar{s}/2}(s^{(c)}) = 0.24$	42.31° $\delta_{\Lambda_{c/4}}(s^{(c)}) = 0.18$

Table IV. Comparison of the first five natural frequencies (in Hz) of the three "test" design points delivered by the generalized interpolation method with their counterparts obtained from direct ROM constructions.

	Test design point (a)			Test design point (b)			Test design point (c)		
Mode	Direct ROM	Interp. ROM	Relative discrepancy	Direct ROM	Interp. ROM	Relative discrepancy	Direct ROM	Interp. ROM	Relative discrepancy
1	9.11	9.00	1.2 %	14.5	14.8	2.1 %	12.3	12.8	4.1 %
2	35.4	35.1	0.8 %	51.7	53.4	3.3 %	41.2	42.5	3.2 %
3	44.7	43.9	1.8 %	72.8	73.8	1.4 %	61.9	63.9	3.2 %
4	88.6	87.7	1.0 %	128	131	2.7 %	107	110	2.8 %
5	117	117	0.0 %	186	186	0.0 %	158	164	3.7 %

Table V. Modal Assurance Criterion (MAC) applied to the interpolated mode shapes and their counterparts obtained from direct ROM constructions.

Mode	MAC for test design point (a)	MAC for test design point (b)	MAC for test design point (c)
1	1.0000	1.0000	1.0000
2	0.9999	0.9994	0.9985
3	0.9999	0.9998	0.9993
4	0.9995	0.9995	0.9986
5	0.9702	0.9504	0.9962

Table VI. Relative discrepancies between the maximum amplitude of the vertical displacement at the trailing edge tip predicted by the complete FEM, the directly computed ROMs and the interpolated ROMs.

Test design point (a)		Test design point (b)		Test design point (c)	
Direct ROM	Interp. ROM	Direct ROM	Interp. ROM	Direct ROM	Interp. ROM
1.87%	8.67%	2.77%	7.77%	3.30%	7.98%

uniformly distributed vertical load. For this purpose, three simulations are performed for each test design configuration using: (a) the full-order FEM dynamic model, (b) a ROM counterpart directly built from the first five natural modes of this model and (c) the ROM counterpart computed by interpolating the 17 quintuplets stored in the ROM database. In all cases, the governing equations of dynamic equilibrium are time-integrated by the trapezoidal rule. Figure 6, Figure 7 and Figure 8 report for the test design points $s^{(a)}$, $s^{(b)}$ and $s^{(c)}$, respectively, the computed time-histories of the vertical displacement at the trailing edge tip point of the wing using each of the three different computational models. The reader can observe that in each case, the interpolated ROM delivers good accuracy. Indeed, Table VI shows that in each case, the relative discrepancy between the maximum amplitudes of the dynamic responses predicted by the full-order FEM and interpolated ROM is of the order of 8% only. For comparison, the relative discrepancy between the maximum amplitudes of the dynamic responses predicted by the full-order FEM and directly computed ROM is of the order of 3%.

5. CONCLUSIONS

A rigorous method for interpolating parameterized linear structural dynamics reduced-order models (ROMs) has been presented. The main purpose of this method is to construct in real-time a new ROM for every new set of values of the given parameters. This method operates only on the ROMs themselves and not on the underlying full-order models. Hence, it is amenable to an on-line implementation. Its robustness and accuracy have been demonstrated for the fast dynamic characterization of a parameterized mechanical system and prediction of the transient

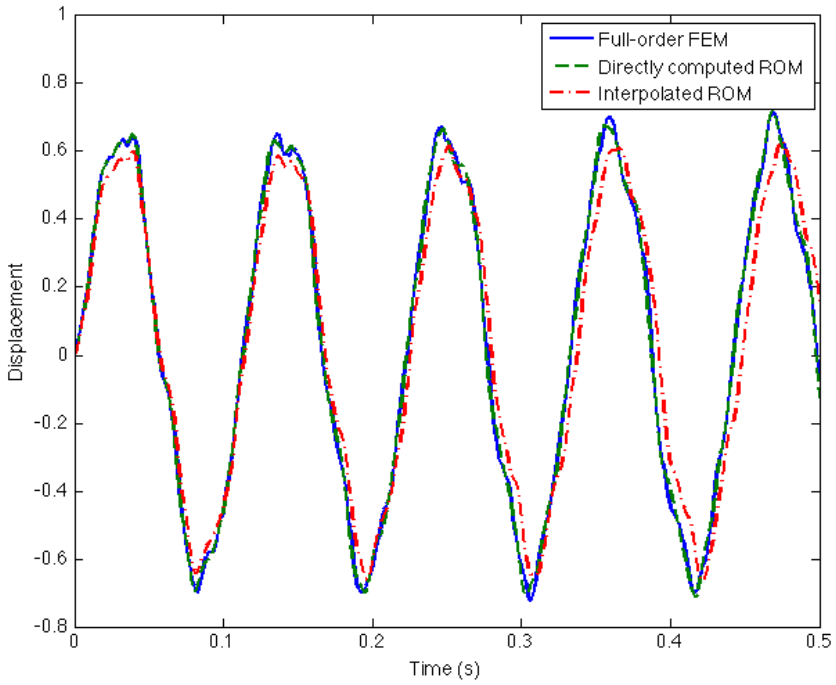

Figure 6. Test design point $s^{(a)}$: transient responses predicted by the complete FEM model, the directly computed ROM and the interpolated ROM.

response of another one to a given input. This interpolation method is particularly appealing for structural dynamics optimization procedures in which ROMs are used as surrogate models.

6. APPENDIX

Here, an important proposition characterizing the proposed generalized interpolation method in a tangent space to a matrix manifold is proven. For this purpose, it is assumed that the generalized interpolation method is equipped with a standard multi-variate interpolation algorithm that approximates constant functions exactly (for example, see[18]).

Proposition. Let $S = \left(s^{(0)}, s^{(1)}, \ldots, s^{(N_R-1)}\right)$ denote a set of N_R operating points and let $\left\{R_i = (I_n,\ C_i^\star,\ \Omega_{n,i}^2)\right\}_{i=0}^{N_R-1}$ denote a corresponding set of N_R triplets representing N_R parameterized linear structural dynamics *modal* ROMs of size $n << N$ each, where $I_n = I\left(s^{(i)}\right) \in \mathbb{R}^{n\times n}$ is the identity matrix of size n, $C_i^\star = C^\star\left(s^{(i)}\right) \in \mathbb{R}^{n\times n}$ is positive definite and $\Omega_{n,i}^2 = \Omega_n^2\left(s^{(i)}\right) \in \mathbb{R}^{n\times n}$ is a diagonal matrix with n positive entries representing

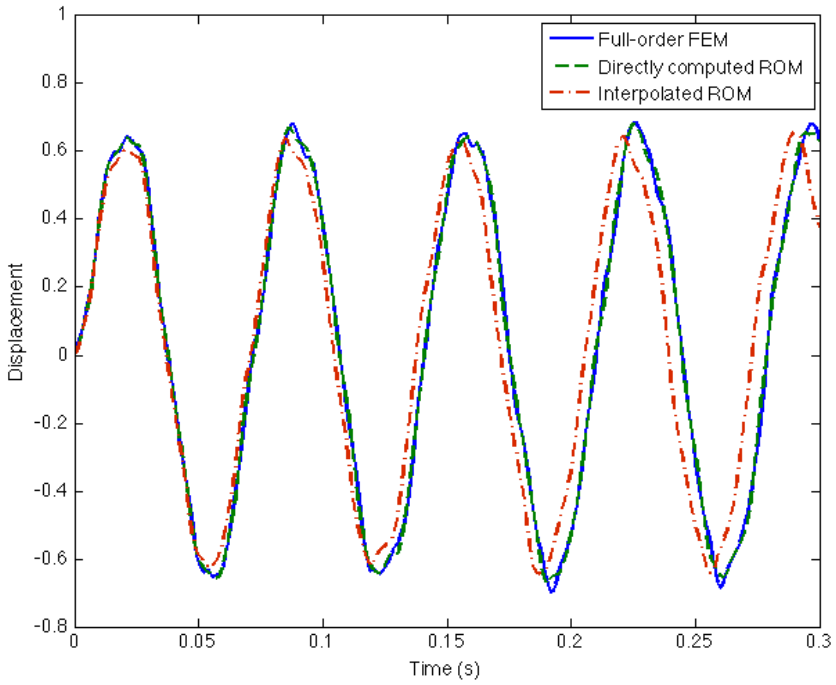

Figure 7. Test design point $s^{(b)}$: transient responses predicted by the complete FEM model, the directly computed ROM and the interpolated ROM.

the squares of n natural circular frequencies

$$\Omega^2_{n,i} = \begin{bmatrix} \omega^2_{1,i} = \left(\omega_1\left(s^{(i)}\right)\right)^2 & & 0 \\ & \omega^2_{2,i} = \left(\omega_2\left(s^{(i)}\right)\right)^2 & \\ & & \ddots \\ 0 & & \omega^2_{n,i} = \left(\omega_n\left(s^{(i)}\right)\right)^2 \end{bmatrix}. \tag{24}$$

Given a new operating point $s^{(N_R)} \notin S$, the generalized interpolation method described in Section 3.1 of this paper delivers a triplet of the form $R_{N_R} = (I_n,\ C^{\star}_{N_R},\ \Omega^2_{n,N_R})$, where Ω^2_{n,N_R} is a diagonal matrix with n positive entries.

Proof. In this case, the step-by-step application of the generalized interpolation method presented in Section 3.1 to the set of N_R SPD matrices $I\left(s^{(i)}\right) = I_n$ gives the following results.

- Step 0. $I\left(s^{(i_0)}\right) = I_n$ is chosen as a reference element of SPD(n).
- Step 1. Each element $I\left(s^{(i)}\right) = I_n$ is obviously close to itself and therefore is mapped to the matrix Γ_i of $\mathcal{T}_{I_n}\mathrm{SPD}(n)$ as follows

$$\Gamma_i = \mathrm{Log}_{I_n}(I_n) = \mathtt{log}\left({I_n}^{-1/2} I_n I_n^{-1/2}\right) = \mathtt{log}\left(I_n\right) = 0_n \tag{25}$$

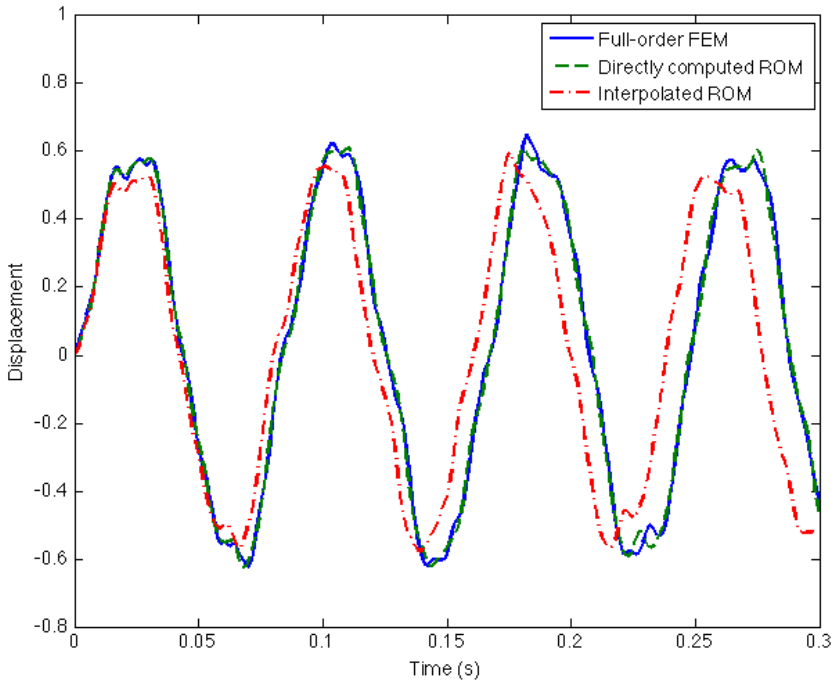

Figure 8. Test design point $s^{(c)}$: transient responses predicted by the complete FEM model, the directly computed ROM and the interpolated ROM.

where 0_n denotes the zero square matrix of size n.

- Step 2. Each entry of the matrix Γ_{N_R} associated with the target operating point $s^{(N_R)}$ is computed by interpolating the corresponding entries of the matrices $\{\Gamma_i = 0_n\}_{i=0}^{N_R-1}$ associated with the operating points $\{s^{(i)}\}_{i=0}^{N_R-1}$. Since a standard interpolation algorithm approximates exactly a constant fonction,

$$\Gamma_{N_R} = 0_n. \tag{26}$$

- Step 3. The matrix $\Gamma_{N_R} \in \mathcal{T}_{I_n}\mathrm{SPD}(n)$ is mapped to a matrix $M^{\star}_{N_R} \in \mathrm{SPD}(n)$ as follows

$$M^{\star}_{N_R} = \mathrm{Exp}_{I_{i_0}}(\Gamma_{N_R}) = {I_n}^{1/2}\mathtt{exp}(\Gamma_{N_R}){I_n}^{1/2} = \mathtt{exp}(0_n) = I_n, \tag{27}$$

which proves the first part of the above proposition.

Similarly, the step-by-step application of the generalized interpolation method presented in Section 3.1 to the set of N_R SPD matrices $\Omega^2_{n,i}$ (24) gives the following results.

- Step 0. $\Omega^2_{i_0}$ is chosen as a reference element of $\mathrm{SPD}(n)$.

- Step 1. Each matrix Ω_i^2 that is sufficiently close to $\Omega_{i_0}^2$ is mapped to a matrix Γ_i of $\mathcal{T}_{\Omega_{i_0}^2}\mathrm{SPD}(n)$ as follows

$$
\begin{aligned}
\Gamma_i &= \mathrm{Log}_{\Omega^2_{n,i_0}}(\Omega^2_{n,i}) \\
&= \mathtt{log}\left({\Omega^2_{n,i_0}}^{-1/2}\Omega^2_{n,i}{\Omega^2_{n,i_0}}^{-1/2}\right) \\
&= \mathtt{log}\left(\begin{bmatrix} \omega_{1,i_0}^{-1} & & & 0 \\ & \omega_{2,i_0}^{-1} & & \\ & & \ddots & \\ 0 & & & \omega_{n,i_0}^{-1} \end{bmatrix}\begin{bmatrix} \omega_{1,i}^{2} & & & 0 \\ & \omega_{2,i}^{2} & & \\ & & \ddots & \\ 0 & & & \omega_{n,i}^{2} \end{bmatrix}\begin{bmatrix} \omega_{1,i_0}^{-1} & & & 0 \\ & \omega_{2,i_0}^{-1} & & \\ & & \ddots & \\ 0 & & & \omega_{n,i_0}^{-1} \end{bmatrix}\right) \\
&= \mathtt{log}\left(\begin{bmatrix} \left(\frac{\omega_{1,i}}{\omega_{1,i_0}}\right)^2 & & & 0 \\ & \left(\frac{\omega_{2,i}}{\omega_{2,i_0}}\right)^2 & & \\ & & \ddots & \\ 0 & & & \left(\frac{\omega_{n,i}}{\omega_{n,i_0}}\right)^2 \end{bmatrix}\right) \\
&= \begin{bmatrix} 2\log\left(\frac{\omega_{1,i}}{\omega_{1,i_0}}\right) & & & 0 \\ & 2\log\left(\frac{\omega_{2,i}}{\omega_{2,i_0}}\right) & & \\ & & \ddots & \\ 0 & & & 2\log\left(\frac{\omega_{n,i}}{\omega_{n,i_0}}\right) \end{bmatrix}.
\end{aligned} \tag{28}
$$

- Step 2. Each entry of the matrix Γ_{N_R} associated with the target operating point $s^{(N_R)}$ is computed by interpolating the corresponding entries of the matrices $\{\Gamma_i\} \in \mathbb{R}^{n\times n}$ associated with the operating points $\{s^{(i)}\}$. Since each matrix Γ_i (28) is in this case diagonal, Γ_{N_R} is also diagonal and can be written as

$$
\Gamma_{N_R} = \begin{bmatrix} \alpha_1 & & & 0 \\ & \alpha_2 & & \\ & & \ddots & \\ 0 & & & \alpha_n \end{bmatrix}. \tag{29}
$$

- Step 3. The matrix $\Gamma_{N_R} \in \mathcal{T}_{\Omega^2_{n,i_0}}\mathrm{SPD}(n)$ is mapped to a matrix $K^\star_{N_R}$ on $\mathrm{SPD}(n)$ as

follows

$$
\begin{aligned}
K^{\star}_{N_R} &= \mathrm{Exp}_{\Omega^2_{n,i_0}}(\Gamma_{N_R}) \\
&= {\Omega^2_{n,i_0}}^{1/2} \mathsf{exp}(\Gamma_{N_R}) {\Omega^2_{n,i_0}}^{1/2} \\
&= \begin{bmatrix} \omega_{1,i_0} & & & 0 \\ & \omega_{2,i_0} & & \\ & & \ddots & \\ 0 & & & \omega_{n,i_0} \end{bmatrix} \begin{bmatrix} \exp(\alpha_1) & & & 0 \\ & \exp(\alpha_2) & & \\ & & \ddots & \\ 0 & & & \exp(\alpha_n) \end{bmatrix} \\
&\quad \begin{bmatrix} \omega_{1,i_0} & & & 0 \\ & \omega_{2,i_0} & & \\ & & \ddots & \\ 0 & & & \omega_{n,i_0} \end{bmatrix} \\
&= \begin{bmatrix} \omega^2_{1,i_0}\exp(\alpha_1) & & & 0 \\ & \omega^2_{2,i_0}\exp(\alpha_2) & & \\ & & \ddots & \\ 0 & & & \omega^2_{n,i_0}\exp(\alpha_n) \end{bmatrix} \\
&= \begin{bmatrix} \omega^2_{1,N_R} & & & 0 \\ & \omega^2_{2,N_R} & & \\ & & \ddots & \\ 0 & & & \omega^2_{n,N_R} \end{bmatrix} = \Omega^2_{n,N_R},
\end{aligned}
$$

which proves the second and last part of the above proposition.

ACKNOWLEDGEMENTS

This material is based upon work supported partially by the Air Force Office of Scientific Research under Grant F49620-01-1-0129 and partially by the National Science Foundation under Grant CNS-0540419. Any opinions, findings and conclusions or recommendations expressed in this material are those of the authors and do not necessarily reflect the views of the Air Force Office of Scientific Research or the National Science Foundation.

REFERENCES

1. Guyan RJ. Reduction of stiffness and mass matrices. *AIAA Journal* 1965; **3**(2):380.
2. Flanigan CC. Development of the IRS component dynamic reduction method for substructure analysis. *AIAA Paper 1991-1056* 1991.
3. Holmes P, Lumley J, Berkooz G. *Turbulence, Coherent Structures, Dynamical Systems and Symmetry.* Cambridge University Press, 1996.
4. Kerschen G, Golinval JC, Vakakis AF, Bergman LA. The method of proper orthogonal decomposition for dynamical characterization and order reduction of mechanical systems: an overview. *Nonlinear dynamics* 2005; **41**:147–169.
5. Amabili M, Sarkar A, Paidoussis MP. Reduced-order models for nonlinear vibrations of cylindrical shells via the proper orthogonal decomposition method. *Journal of Fluids and Structures* 2003; **18**(2): 227–250.

6. Han S, Feeny BF. Enhanced proper orthogonal decomposition for the modal analysis of homogeneous structures. *Journal of Vibration and Control* 2002; **8**(1):19–40.
7. Leibfritz F, Volkwein S. Reduced-order Output Feedback Control Design for PDE Systems Using Proper Orthogonal Decomposition and Nonlinear Semidefinite Programming. *Linear Algebra and its Applications, Special Issue on Order Reduction of Large-Scale Systems* 2004; **415**(2–3):542–575.
8. Georgiou IT, Schwartz IB. Dynamics of large scale coupled structural/mechanical systems: a singular perturbation/proper orthogonal decomposition approach. *SIAM Journal of Applied Mathematics* 2002; **59**(4):1178–1207.
9. Hinze M, Volkwein S. Proper orthogonal decomposition surrogate models for nonlinear dynamical systems: error estimates and suboptimal control. In *Dimension Reduction of Large-Scale Systems, Lecture Notes in Computational Science and Engineering,* Springer **45**, 2006; 261–306.
10. Danowsky B, Chrstos J, Klyde D, Farhat C, Brenner M. Application of multiple methods for aeroelastic uncertainty analysis. *AIAA Paper 2008-6371, AIAA Atmospheric Flight Mechanics Conference and Exhibit*, Honolulu, Hawaii, August 18-21, 2008.
11. Amsallem D, Farhat C. An interpolation method for adapting reduced-order models and application to aeroelasticity. *AIAA Journal* 2008; **46**(7):1803–1813.
12. Epureanu BI. A parametric analysis of reduced order models of viscous flows in turbomachinery. *Journal of Fluids and Structures* 2003; **17**(7):971–982.
13. Amsallem D, Cortial J, Farhat C. On-demand CFD-based aeroelastic predictions using a database of reduced-order bases and models. *AIAA Paper 2009-800, 47th AIAA Aerospace Sciences Meeting including The New Horizons Forum and Aerospace Exposition,* Orlando, Florida, Jan. 5-8, 2009.
14. Pennec X, Fillard P, Ayache N. A Riemannian framework for tensor computation. *International Journal of Computer Vision* 2006; **66**(1):41–66.
15. Kim T. Frequency-domain Karhunen-Loeve method and its application to linear dynamic systems. *AIAA Journal* 1998; **36**(11):2117–2123.
16. Yates EC. Agard standard aeroelastic configurations for dynamic response, candidate configuration I, -Wing 445.6. *NASA TM-100462* 1987.
17. Ewins DJ. *Modal Testing, Theory, Practice and Application* (2nd edn). Research Study Press LTD, 2000.
18. Späth H. *Two Dimensional Spline Interpolation Algorithms.* K Peters, Ltd., 1995.